I&EC research
Industrial & Engineering Chemistry Research

Article

Cite This: Ind. Eng. Chem. Res. XXXX, XXX, XXX−XXX

pubs.acs.org/IECR

Modeling of Trifluoromethane (R-23) or Hexafluoroethane (R-116) and Alkane Binary Mixtures using the Group-Contribution with Association Equation of State

Mark D. Williams-Wynn,[†] Francisco Adrián Sánchez,[‡] Paramespri Naidoo,[†] Selva Pereda,*[,†,‡] and Deresh Ramjugernath[†]

[†]Thermodynamics Research Unit, School of Engineering, University of KwaZulu-Natal, Howard College Campus, King George V Avenue, Durban 4041, South Africa

[‡]Planta Piloto de Ingeniería Química (PLAPIQUI), Universidad Nacional del Sur (UNS) - CONICET, Camino La Carrindanga Km7, 8000B Bahía Blanca, Argentina

ABSTRACT: The group-contribution with association equation of state (GCA-EOS) has been applied to represent the phase behavior of binary systems containing either trifluoromethane (R-23) or hexafluoroethane (R-116) with alkanes. The model was successfully fitted to selected literature data, which also formed part of a study into the use of these refrigerants as supercritical fluid extraction solvents. The tuned model was tested against the available experimental data covering the homologous series of C_2 to C_{11} alkanes with either R-23 or R-116, at temperatures between 193 and 343 K and at pressures of up to 60 MPa. The tuned model provided accurate predictions of the phase behavior of these systems, including the ability to identify the carbon number of the alkane in the system at which the phase equilibria transformation occurred. The comparison of the model to the experimental data was excellent, with absolute average relative deviations of between 1% and 5% for both pressure and vapor phase compositions.

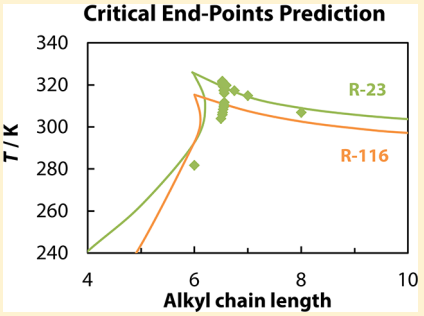

1. INTRODUCTION

In recent years, investigations into the performance of supercritical fluorinated refrigerants as solvents for the separation of oil sludges were undertaken,[1−7] chiefly through measuring the phase equilibrium data for binary systems. Supercritical fluid extraction (SCFE) using fluorinated refrigerants, rather than the more commonly used carbon dioxide, was investigated by Williams-Wynn et al.[4,5,8] In general, the addition of a cosolvent, such as ethanol, to supercritical carbon dioxide improves the performance of the extraction.[9,10] However, the addition of a cosolvent complicates the solvent recovery process and adds additional purification steps. The aim of using alternative fluorinated solvents was to prevent the need for the addition of a cosolvent to enhance the solubilities for the SCFE. Trifluoromethane (R-23) and hexafluoroethane (R-116) were the two SCFE solvents proposed for use in the supercritical extraction of hydrocarbon mixtures.[6] The chief reasons behind their proposal of these fluorinated compounds are their favorable critical properties and, in the case of R-23, the convenient dipole moment given by its asymmetric structure.

The binary systems for which experimental data were available consist mainly of normal alkanes, with alkyl chain lengths of between 2 and 11 carbon atoms, and one of the refrigerants. The phase equilibrium data were measured using a high pressure vapor−liquid equilibria (VLE) apparatus. However, VLE measurements are time-consuming tasks, making it virtually impossible to measure the data for every binary combination that could possibly exist with the hydrocarbons being studied. Therefore, a predictive thermodynamic model, tunable to the equilibrium data of a few measured systems, may provide a faster means of understanding the behavior of the homologous series containing alkanes. Moreover, a predictive model can be particularly useful because, as the chain length of the *n*-alkanes becomes longer, the systems become more difficult to analyze in high pressure cells. This is primarily due to the increased viscosities and decreased volatilities with increases in chain length of the molecules. As most sampling techniques for high pressure VLE rely on capillaries or microvalves,[11] together with the vaporization of the samples for GC analysis, increased sample viscosities, coupled with decreased volatilities, result in impaired composition analysis. An alternative for the measurement of the VLE of systems containing a liquid with a high viscosity is a static-synthetic apparatus. However, for this technique, only the composition of the entire contents of the cell is known, and the compositions of the individual phases cannot be determined analytically. Notwithstanding this, the coupling of these measurements to the use of a predictive thermodynamic model can enable a good understanding of the system despite not obtaining a full $P-x-y$ data set for each system. Moreover, a predictive model allows not

Received: May 3, 2018
Revised: June 29, 2018
Accepted: July 5, 2018
Published: July 5, 2018

DOI: 10.1021/acs.iecr.8b01933
Ind. Eng. Chem. Res. XXXX, XXX, XXX−XXX

only for data interpolation but also for the prediction of the phase behavior of the systems under a broader set of conditions.

Several authors have recognized the importance of considering the comprehensive phase behavior in order to develop predictive thermodynamic models and have made efforts to describe the phase behavior transition of homologues series using group-contribution models,[12,13] generalized correlations,[14−17] or transferable parameters.[18,19] Most of the efforts have been applied to mixtures involving carbon dioxide, with a notable exception being the work of Polishuk[20] who studied the tetrafluoromethane + alkanes homologues series. Nonetheless, to our knowledge, a comprehensive study of the homologues series involving R-23 or R-116 has not been done so far.

Recently, González Prieto et al. presented a parametrization strategy to model multiphase behavior, which included carbon dioxide + alkanes[12] and alkanol[13] homologues series, up to 36 carbon atoms. Using the Group Contribution with Association equation of state (GCA-EOS) with a single set of parameters, the authors assessed the phase behavior transition of both homologous series with CO_2 simultaneously, while obtaining accurate predictions of most of the experimental VLE and LLE data. Sánchez et al.[21] described some of the applications for which the GCA-EOS has been used. One of the more apt applications of the GCA-EOS for this study was the investigation into the optimal design of supercritical fluid processes using the GCA-EOS by Espinosa et al.[22,23] The ability of the model to describe supercritical processes makes it a suitable model to use for the design of a method using supercritical fluorinated refrigerants to process alkanes.

The GCA-EOS assigns parameters to the various groups that make up the molecules, with the sum of the individual contributions resulting in the prediction of the behavior of the system.[24] This technique is a useful tool for the prediction of the thermodynamic behavior of a series of homologous binary systems, as the simple "addition of a group" to a molecule gives a prediction of a different system in the series. Therefore, in this work the parameters for the GCA-EOS were tuned for the trifluoromethane (R-23) and hexafluoroethane (R-116) molecules with the *n*-alkanes being made up of CH_3 and CH_2 groups. This thermodynamic model then enables the prediction of the behavior of numerous other *n*-alkanes with the studied refrigerants.

2. THERMODYNAMIC MODELING

2.1. GCA-EOS Model. The GCA-EOS[24] consists of three contributions to the residual Helmholtz energy (A^R) term: the free volume (A^{fv}), the attractive (A^{att}) and the association (A^{assoc}) terms, where

$$A^R = A^{fv} + A^{att} + A^{assoc} \tag{1}$$

The free volume contribution to the residual Helmholtz energy based on the Carnahan−Starling equation[25] for mixtures of hard spheres as proposed by Mansoori and Leland[26] can be estimated

$$\frac{A^{fv}}{RT} = 3\frac{\lambda_1\lambda_2}{\lambda_3}(Y-1) + \frac{\lambda_2^3}{\lambda_3^2}(Y^2 - Y - \ln Y) + n\ln Y \tag{2}$$

with

$$Y = \left(1 - \frac{\pi\lambda_3}{6V}\right)^{-1} \tag{3}$$

$$\lambda_k = \sum_{i=1}^{NC} n_i d_i^k \qquad k = 1, 2, 3 \tag{4}$$

In eq 2, d_i and n_i are the hard-sphere diameter and the number of moles of component *i*, respectively. NC is the number of components, *R* is the universal gas constant, *T* is the temperature, and *V* is the total volume.

The generalized expression[24]

$$d_i = 1.065655 d_{ci}\left[1 - 0.12\exp\left(\frac{-2T_{ci}}{3T}\right)\right] \tag{5}$$

gives the temperature dependence of the hard sphere diameter, where d_{ci} and T_{ci} are the critical hard sphere diameter and the critical temperature of component *i*, respectively.

The attractive contribution to eq 1, A^{att}, accounts for the attractive forces between the defined functional groups present in the mixture. It includes dispersion forces, as well as dipole and quadrupole interactions. This is a van der Waals term coupled with a density dependent local-composition mixing rule based on a group contribution version of the NRTL model.[27] After integrating the van der Waals equation of state (VDW-EOS) for a pure compound, $A^{att}{}_i(T,V) = -a_i n_i \rho_i$, with ρ_i, the molar density of component *i*.

The energy parameter, *a*, can be determined as follows:

$$a = \frac{z}{2} q^2 g \tag{6}$$

where *g* is defined as the characteristic attractive energy per surface and *q* is the number of surface segments, as defined by the UNIFAC method.[28] In these interactions, which are assumed to take place through the surface, the coordination number (z) is set to 10. When extended to mixtures, the GCA-EOS uses the local surface fractions rather than local mole fractions, in a manner similar to that in the UNIQUAC model.[29] Then, the attractive contribution in eq 1 becomes

$$\frac{A^{att}}{RT} = -\frac{\frac{z}{2}\tilde{q}^2 g_{mix}}{RTV} \tag{7}$$

where $\tilde{q}$ is the total number of surface segments, calculated using eq 8, and g_{mix} is the characteristic attraction energy per total segments, which is calculated using eq 9.

$$\tilde{q} = \sum_{i=1}^{NC}\sum_{j=1}^{NG} n_i \nu_{ij} q_j \tag{8}$$

$$g_{mix} = \sum_{j=1}^{NG} \theta_j \sum_{k=1}^{NG} \frac{\theta_k \tau_{kj} g_{kj}}{\sum_{l=1}^{NG} \theta_l \tau_{lj}} \tag{9}$$

In eqs 8 and 9, v_{ij} is the number of *j*-type groups in molecule *i*, q_j is the number of surface segments assigned to group *j*, and θ_j is the surface fraction of group *j*. In addition,

$$\theta_j = \frac{1}{\tilde{q}} \sum_{i=1}^{NC} n_i \nu_{ij} q_j \tag{10}$$

$$\tau_{kj} = \exp\left[\alpha_{kj}\frac{\tilde{q}(g_{kj} - g_{jj})}{RTV}\right] \tag{11}$$

In eq 9, g_{kj} is the attractive energy between groups *k* and *j* and α_{kj} is the nonrandomness parameter. If a value of zero is assigned

DOI: 10.1021/acs.iecr.8b01933
Ind. Eng. Chem. Res. XXXX, XXX, XXX−XXX

to the nonrandomness parameters, eq 9 reduces to the classic quadratic mixing rule.

The attractive energy term can be calculated through the combination rule presented in eq 12, using the temperature dependent parameters calculated by means of eqs 13 and 14.

$$g_{ij} = k_{ij}\sqrt{g_{ii}g_{jj}} \tag{12}$$

with $k_{ij} = k_{ji}$ and

$$g_{ii} = g_{ii}^{*}\left[1 + g_{ii}^{'}\left(\frac{T}{T_i^{*}} - 1\right) + g_{ii}^{''}\ln\left(\frac{T}{T_i^{*}}\right)\right] \tag{13}$$

$$k_{ij} = k_{ij}^{*}\left[1 + k_{ij}^{'}\ln\left(\frac{2T}{T_i^{*} + T_j^{*}}\right)\right] \tag{14}$$

In particular, g_{ii}^{*} and k_{ij}^{*} are, respectively, the attraction energy and the interaction parameter at the reference temperature, T_i^{*} or $(T_i^{*} + T_j^{*})/2$.

Finally, the association contribution to the residual Helmholz free energy (eq 1), A^{assoc}, is a group contribution version of the association term within the SAFT equation.[30] The calculation of the association term is given by eq 15.

$$\frac{A^{\text{assoc}}}{RT} = \sum_{i=1}^{\text{NGA}} n_i^{*}\left[\sum_{k=1}^{M_i}\left(\ln X_{ki} - \frac{X_{ki}}{2}\right) + \frac{M_i}{2}\right] \tag{15}$$

where NGA is the total number of associating groups, n_i^{*} is the total number of moles of associating group i, calculated as in eq 16, M_i is the number of associating sites in group i, and X_{ki} is the fraction of nonbonded group i, through the site k (eq 17).

$$n_i^{*} = \sum_{m=1}^{\text{NC}} \nu_{mi}^{*} n_m \tag{16}$$

$$X_{ki} = \left(1 + \sum_{j=1}^{\text{NGA}}\sum_{l=1}^{M_j} \frac{n_j^{*} X_{lj}\Delta_{ki,lj}}{V}\right)^{-1} \tag{17}$$

In eq 16, ν_{mi}^{*} is the number of associating groups, i, present in molecule m. Furthermore, in eq 17, X_{kj} is dependent on the association strength between the site k of group i, and the site i of group j ($\Delta_{ki,lj}$), which can be calculated using eq 18.

$$\Delta_{ki,lj} = \kappa_{ki,lj}\left[\exp\left(\frac{\varepsilon_{ki,lj}}{RT}\right) - 1\right] \tag{18}$$

where $\kappa_{ki,lj}$ and $\varepsilon_{ki,lj}$ are the temperature dependent association strengths between the site k of group i and the site l of group j, with regard to association volume and energy parameters, respectively.

2.2. Parameterization Procedure. The regression was performed by the minimization of the objective function, F_{obj}, given by eq 19.

$$F_{\text{obj}} = \sum_{i=1}^{\text{NSat}} {\delta_{\text{sat},i}}^2 + \sum_{i=1}^{\text{NEq}} {\delta_{\text{eq},i}}^2 \tag{19}$$

where NSat and NEq are the number of experimental saturation and binary VLE data points available, and ${\delta_{\text{sat},i}}^2$ and ${\delta_{\text{eq},i}}^2$, are the deviations in the pure component vapor pressure and binary VLE data, which are calculated using eqs 20 and 21.

$${\delta_{\text{sat},i}}^2 = \left(\frac{P_{\text{exp},i}^{\text{sat}} - P_{\text{calc},i}^{\text{sat}}}{P_{\text{exp},i}^{\text{sat}}}\right)^2 \tag{20}$$

$${\delta_{\text{eq},i}}^2 = \text{IFL}_i\left(\frac{P_{\text{exp},i} - P_{\text{calc},i}}{P_{\text{exp},i}}\right)^2 + (1 - \text{IFL}_i)\left(\frac{x_{\text{exp},i} - x_{\text{calc},i}}{x_{\text{exp},i}}\right)^2 + \left(\frac{y_{\text{exp},i} - y_{\text{calc},i}}{y_{\text{exp},i}}\right)^2 \tag{21}$$

In these equations, the P, x, and y terms refer to the pressure and liquid and vapor phase compositions, respectively. IFL is set equal to 0 for TP flash calculation and to 1 for bubble point calculations.

The VLE, liquid−liquid equilibrium (LLE), and vapor−liquid−liquid equilibrium (VLLE) data were regressed by the minimization of the objective function. This was achieved by using the Levenberg−Marquardt finite difference algorithm coded with Fortran77. The correlation procedure was performed in two steps. First, the pure component GCA-EOS group parameters for R-23 and R-116 were regressed from pure vapor pressure data. Thereafter, the alkane-R-23 and alkane-R-116 interaction parameters were regressed using selected high pressure binary equilibrium data.

2.3. Regression of New Groups. Two new groups were defined to enable the description of the fluorinated hydrocarbons with the GCA-EOS. Both the R-23 and the R-116 molecules were defined as single groups. The molecular structures of these compounds are shown in Figure 1.

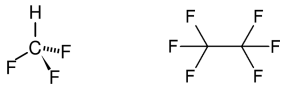

Figure 1. Trifluoromethane (R-23) molecule (left) and hexafluoroethane (R-116) molecule (right).

In the case of molecular groups that do not self-associate, the hard sphere diameter and the group attractive energy (g^{*}), at T_c, can be calculated as it is done with the classic equations of state, as follows:[31]

$$d_c = \sqrt[3]{0.08942656\frac{RT_c}{P_c}} \tag{22}$$

To obtain the attractive energy parameters (g) for the pure groups, the pure component vapor pressures must be fitted with the GCA-EOS, solving for g_i^{*}, $g_i^{'}$, and $g_i^{''}$. The initial estimate for g^{*} can be calculated using

$$g^{*} = g_c = 0.09927761\frac{R^2{T_c}^2}{q^2 P_c} \tag{23}$$

In this work, the logarithmic dependence of eq 13 (g'') was set to zero as is usual for volatile compounds.[32] Therefore, only the linear dependence parameter (g') was fitted to the vapor pressure of pure R-23 or R-116.

2.4. Regression of Binary Mixtures. For the initial estimation of the binary parameters, these were set to their default values, with the predicted phase behavior being that of a classical van der Waals "one-fluid" system (as $k_{ij}^{*} = 1$, and $k_{ij}^{'} = \alpha_{ij} = \alpha_{ji} = 0$). The parametrization was then performed stepwise, first correlating the k_{ij}^{*} alone, and thereafter, the remaining

DOI: 10.1021/acs.iecr.8b01933
Ind. Eng. Chem. Res. XXXX, XXX, XXX−XXX

Table 1. Pure Component Critical Temperatures, T_c,[33] and Diameters, d_c, for the Repulsive Contributions of the GCA-EOS, and the Correlation Statistics (AARD(P^{sat})), for the Prediction of the Vapor Pressures[6,34−43] in the Reduced Temperature Range, ΔT_r

compound	CAS	T_c/K	P/MPa	d_c/cm mol$^{-1/3}$	ΔT_r	AARD(P^{sat})/%[a]
trifluoromethane (R-23)	75-46-7	299.07	4.836	3.5824	0.45−0.99	1.8
hexafluoroethane (R-116)	76-16-4	292.85	2.980	4.1805	0.60−0.98	0.9

[a]Absolute average relative deviation (AARD) for P^{sat}, $\frac{100}{N}\sum_i^N |1 - P^{sat}_{calc,i}/P^{sat}_{exp,i}|$.

Table 2. GCA-EOS Pure Component Parameters for the Attractive Contributions

group i	q_i	T_i^*/K	g_i^*/atm cm^6 mol^{-2}	g_i'	g_i''	ref
CH_3	0.848	600.0	316910	−0.9274	0	32
CH_2	0.540	600.0	356080	−0.8755	0	32
$CHCH_3$	1.076	600.0	303749	−0.8760	0	44
C_2H_6	1.696	305.4	452560	−0.3724	0	32
C_3H_8	2.236	369.8	436890	−0.4630	0	32
CHF_3 (R-23)	1.608	299.07	484409	−0.6272	0	this work
C_2F_6 (R-116)	2.760	292.85	255847	−0.5900	0	this work

parameters were included in successive regressions. If adding a new parameter did not decrease the objective function (eq 19), this parameter was set back to its default value and the next parameter was focused upon. In addition to this procedure, the first regressions were undertaken with the assumption that the interaction parameters between the fluorinated group (CHF_3 or C_2F_3) and the paraffinic groups ($-CH_3$ and $-CH_2-$) were equal. A more detailed explanation of this parametrization procedure is described elsewhere.[12]

3. RESULTS AND DISCUSSION

The results obtained in the calculation of pure and binary phase equilibrium properties with the GCA-EOS model are presented in Tables 1−5. The pure component critical temperatures and diameters for the repulsive contribution to the GCA-EOS are provided in Table 1, alongside the reduced temperature range, ΔT_r, at which they were correlated. The absolute average relative deviations (AARD) of the correlation of the saturated vapor pressures are also presented in Table 1.

The attractive energy parameters for the pure components were fitted for both R-23 and R-116 by using experimental pure component vapor pressures from literature.[6,34−43] Both the pure group parameters fitted to these vapor pressure data and those obtained from literature are presented in Table 2.

An important aspect of using a single model to describe multiple systems with increasing chain length of one of the molecules is its ability to predict the changes in the type of equilibrium occurring, from VLE to VLLE or LLE. Many of the models that have been proposed can predict the phase behavior of binary systems containing a few adjacent members of a homologous series. However, according to González Prieto et al.,[12,13] when the models are extended to systems that have greater differences in the number of atoms in a molecular chain, they perform poorly. González Prieto et al. went on to show that the GCA-EOS with correctly fitted parameters can describe a homologous series well without these problems of false heterogeneous regions that are predicted by other models.

For this work, a databank with about 850 experimental points of the VLE, LLE, and VLLE data of R-23 or R-116 + alkane mixtures was used to parametrize the GCA-EOS model. These data covered a range of temperatures between (193 and 343) K and pressures of up to 9 MPa for the entire VLE data set and up to 60 MPa for the LLE data of R-23 + propane and *n*-butane. Approximately 20% of the database was employed in the correlation process, while the remainder of the data was used solely to test the predictive capabilities of the model.

The final binary interaction parameters obtained from the regression procedure are provided in Table 3. Furthermore,

Table 3. Binary Energy Interaction Parameters for the Attractive Term Fitted in This Work

groups					
i	j	k_{ij}^*	k_{ij}'	α_{ij}	α_{ji}
CHF_3	CH_3	0.8547	0.0473	7.2139	2.5961
	CH_2	0.8864	0.0473	−13.046	−6.7456
	$CHCH_3$	0.8864	0.0473	−13.046	0
	C_2H_6	0.8310	−0.0473	0	0
	C_3H_8	0.8339	−0.0397	0	0
C_2F_6	CH_3	0.8633	0	2.0	−21.85
	CH_2	0.9481	0	−3.12	2.62
	C_2H_6	0.8754	−0.0564	0	0
	C_3H_8	0.8754	−0.0564	0	0

Table 4 shows the resulting errors during the correlation procedure, together with the type of experimental data, temperature, pressure deviations, number of points, and the reference from which the data was obtained. Similarly, Table 5 shows the model performance for the experimental data not included in the regression procedure. The model shows a similar performance in both the correlated and predicted data sets when using only 20% of the total database for the correlation. The absolute average relative deviations (AARD) are about 2% and 1%, respectively, for the bubble pressure and vapor compositions of the binary systems containing R-23. Similarly, AARD of between 1% and 5% were obtained for R-116 binary systems. From these results, it may be argued that the AARD obtained for the VLE of R-116 + *n*-nonane or *n*-decane are rather high. However, as we will show later, the bubble pressure curve of these binary mixtures is rather steep, thus invoking a large change in the bubble pressure with only a small perturbation of the liquid molar fraction.

An important concept that is often considered in the study of homologues series is the change of the system type with increase

DOI: 10.1021/acs.iecr.8b01933
Ind. Eng. Chem. Res. XXXX, XXX, XXX−XXX

Table 4. GCA-EOS Phase Behavior Correlation of Hydrofluorocarbon (HFC) + Hydrocarbon (HC) Binary Systems

Vapor−Liquid Equilibria							
				AARD/%[a]			
HFC	alkane	T/K	P/MPa	P	y_1	no. of exp points	ref
R-23	ethane	188, 244	0.08−1.6	0.76	2.3	16	45
	propane	283, 293, 353	0.63−5.1	1.2	2.1	30	6, 38
	isobutane	283	0.22−3.2	1.1	0.51	9	46
	n-hexane	273, 313	0−5.7	1.1	0.54	17	4
	n-heptane	273, 303	0.01−5.7	1.2	0.4	20	5
	n-undecane	303	0.78−5.3	6.4		8	8
R-116	ethane	189, 253	0.07−1.7	0.36	1.7	17	47
	propane	263, 323	0.44−1.4	0.93	1.4	20	1
	n-butane	296	0.23−2.9	3.8	1.7	8	2
	n-hexane	296	0.02−2.6	5.1	0.25	10	3
	n-decane	293	1.00−2.3	15	0.7	5	8
Vapor−Liquid−Liquid and Liquid−Liquid Equilibria							
				AAD[b] (AARD/%[a]) of x_i in j			
HFC	alkane	T/K	P/MPa	HFC in HC	HC in HFC	no. of exp points	ref
R-23	propane	203−215	20	0.035 (14)	0.023 (27)	3/4	48
	n-heptane	273−313	2.4−5.7	0.011 (2.7)	0.028 (54)	4	5

[a]Average absolute relative deviation relative to Z, $\frac{100}{N}\sum_i^N |1 - Z_{\mathrm{calc},i}/Z_{\mathrm{exp},i}|$. [b]Average absolute deviation in variable Z: $\frac{1}{N}\sum_i^N |Z_{\mathrm{exp},i} - Z_{\mathrm{calc},i}|$.

Table 5. GCA-EOS Phase Behavior Prediction of hydrofluorocarbon (HFC) + Hydrocarbon (HC) Binary Systems

Vapor−Liquid Equilibria							
				AARD/%[a]			
HFC	alkane	T/K	P/MPa	P	y_1	no. of exp points	ref
R-23	ethane	193−229	0.10−1.0	0.80	2.0	40	45
	propane	298−323	0.90−4.4	1.2	1.4	57	6, 38
	isobutane	293.15	0.30−4.1	1.3	1.0	18	46
	n-butane	283−313	0.15−4.7	1.7	1.5	41	2
	isopentane	310, 343	0.54−6.8	2.3	1.8	25	49
	n-pentane	310, 343	0.53−7.1	7.9	1.5	26	49
	n-hexane	283−303	0.01−4.9	1.2	0.63	30	4
	n-heptane	283−293, 313	0−5.7	1.8	0.85	34	5
	n-nonane	273−313	0−6.2	2.7	0.17	61	8
	n-decane	293−323	0−7.8	3.6		46	8
	n-undecane	293, 313, 323	0−9.0	4.4		25	8
R-116	ethane	193, 248	0.09−1.4	0.43	1.7	18	47
	propane	283−308	0.80−3.4	0.87	2.1	45	1
	n-butane	273−323	0.10−3.7	4.3	1.3	55	2
	n-pentane	288, 297	0.31−3.0	2.1	0.54	17	3
	n-hexane	288	0.31−2.2	5.8	0.38	8	3
	n-heptane	293−323	0.01−4.1	4.0		40	5
	n-octane	293−323	0−5.5	5		18	50
	n-nonane	293−323	0−4.7	9		37	8
	n-decane	303−313	0.90−5.4	17	0.46	15	8
Vapor−Liquid−Liquid and Liquid−Liquid Equilibria							
				AAD[b] (AARD/%[a]) of x_i in j			
HFC	alkane	T/K	P/MPa	HFC in HC	HC in HFC	no. of exp points	ref
R-23	propane	210−224	60	0.037 (14)	0.053 (33)	7	48
	butane	227−250	20, 60	0.045 (13)	0.029 (20)	8/12	48
	n-nonane	273−303	2.5−5	0.004 (1.6)	0.006 (38)	4	8
	n-decane	293, 303	4.2−4.8	0.013 (4.1)		2	8

[a]Average absolute relative deviation relative to Z, $\frac{100}{N}\sum_i^N |1 - Z_{\mathrm{calc},i}/Z_{\mathrm{exp},i}|$. [b]Average absolute deviation in variable Z: $\frac{1}{N}\sum_i^N |Z_{\mathrm{exp},i} - Z_{\mathrm{calc},i}|$.

in the alkyl chain length. These system types are commonly defined using the nomenclature proposed by van Konynenberg and Scott.[51] For the phase equilibria transformation of the homologues series that were studied in this work, the only experimental data that are available, to our knowledge, are those for R-23 with alkanes measured by Poot and de Loos.[52] In the published work the homologues series changes from Type II to III between *n*-hexane and *n*-heptane. Contrary to the homologous series

DOI: 10.1021/acs.iecr.8b01933
Ind. Eng. Chem. Res. XXXX, XXX, XXX−XXX

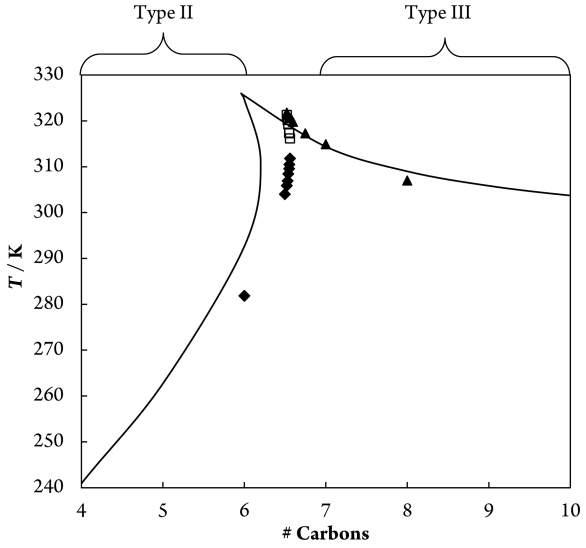

Figure 2. Transformation between types of fluid phase behavior of R23 + *n*-alkane binary systems. Symbols: experimental data of UCEP (◆,▲) and LCEP (□).[52] Lines: GCA-EOS predictions from this work.

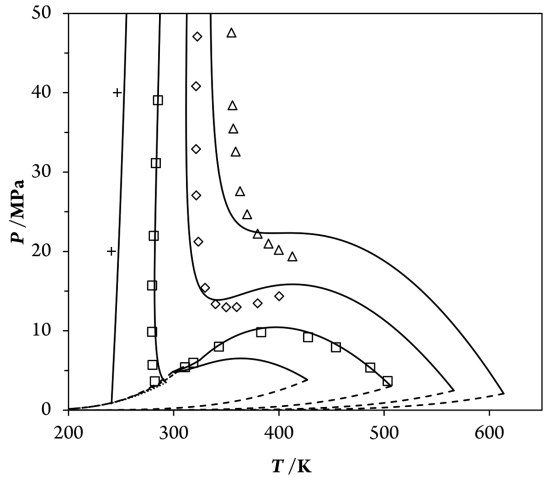

Figure 3. *P*−*T* projection of the phase equilibria of R-23 + *n*-alkanes homologues series. Symbols: experimental data for (+) *n*-butane, (□) *n*-hexane, (◇) *n*-octane, and (△) *n*-decane.[48,55] Lines are GCA-EOS predictions: short dash, pure vapor pressure; solid, predicted critical locus; long dash, binary VLLE.

of CO_2 with *n*-alkanes[53] or *n*-alcohols,[54] there is no Type IV (intermediate) binary system for R-23 + *n*-alkanes. Figure 2 compares the upper and lower critical end points as the alkyl length increases, comparing the experimental data against results obtained with the GCA-EOS in this work. The predicted phase transition that was obtained from the model differs from the experimental data by less than one carbon number. This means that the GCA-EOS can predict the type of phase behavior of R-23 with different *n*-alkanes. The proximity of the predicted and experimental results is remarkable for a predictive model. It is worth mentioning that a better description of the phase transition could have been obtained if desired; however, this would have resulted in a poorer performance of the model in the representation of the overall bubble pressures of the homologous series.

Figure 3 shows the GCA-EOS prediction of the critical loci of selected R-23 + *n*-alkane binary systems, which can be considered a good description for the entire portion of the series that was considered. On the basis of this good description of the *PT* projection of the global phase behavior with increases in the alkyl chain length, it can be expected that the model will also perform well in multiphase systems, despite being reliant on a single set of parameters.

Figures 4−6 show the performance of the model for the high pressure VLE and VLLE of R-23 + alkanes, with varying alkyl chain

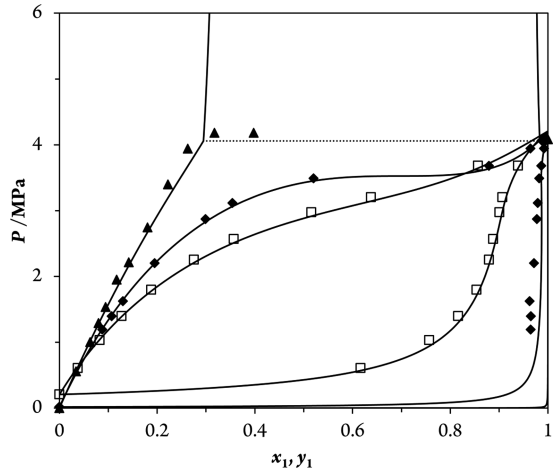

Figure 4. Phase behavior of R-23 (1) + selected *n*-alkane (2) binary systems at 293 K. Symbols: experimental data of (□) *n*-butane,[38] (◆) *n*-hexane,[4] and (▲) *n*-decane.[8] Lines: solid, prediction with the GCA-EOS (this work); dotted, correlated and predicted VLLE (this work).

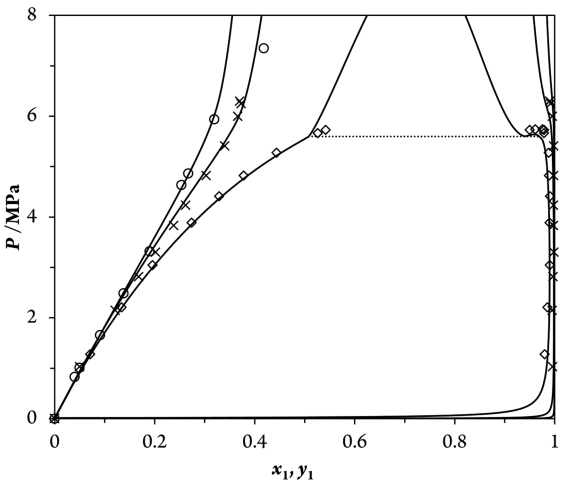

Figure 5. Phase behavior of R-23 (1) + selected *n*-alkane (2) binary systems at 313 K. Symbols: experimental data of (◇) *n*-heptane,[5] (×) *n*-nonane,[8] and (○) *n*-undecane.[8] Lines: solid, GCA-EOS prediction (this work); dotted, correlated VLLE (this work).

length and temperature. The model can describe the bubble pressures of the various binary systems accurately, solely through the variance of the number of CH_2 groups in the alkane molecule. Analogously, Figures 7 and 8 show the phase behavior of R-116 with several *n*-alkanes at similar temperatures. As can be seen, the model accurately describes the experimental data that are available for this homologous series. For the systems containing R-116, the GCA-EOS predicts a transition from Type II to Type III at alkyl chain lengths between five and six carbons. This is one

DOI: 10.1021/acs.iecr.8b01933
Ind. Eng. Chem. Res. XXXX, XXX, XXX−XXX

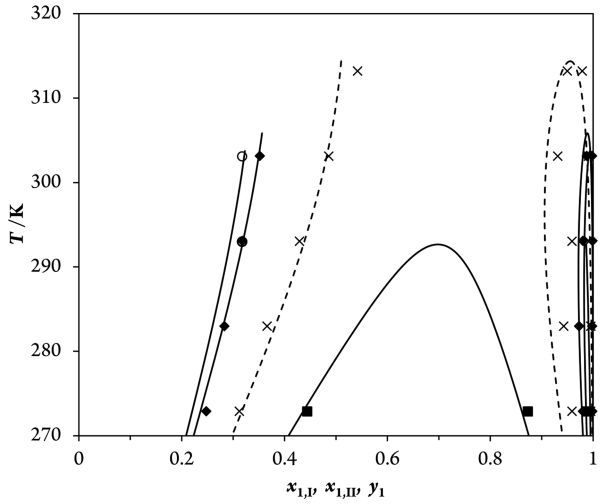

Figure 6. Phase behavior of R-23 (1) + selected *n*-alkane (2) binary systems. Symbols: experimental data of (■) *n*-hexane,[4] (×) *n*-heptane,[5] (◆) *n*-nonane,[8] and (○) *n*-decane.[8] Dashed and solid lines: GCA-EOS correlation and prediction, respectively (this work).

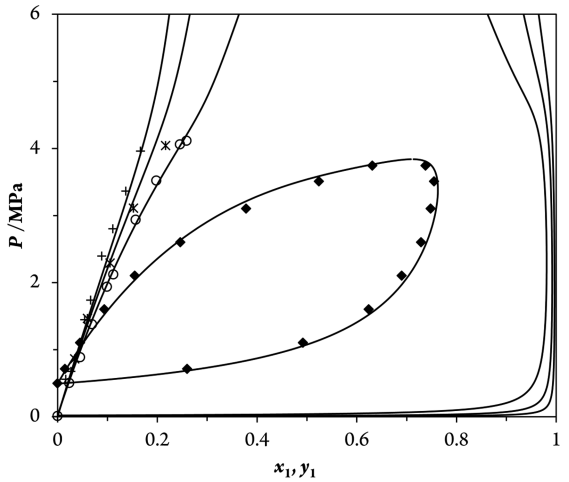

Figure 8. Phase behavior of R-116 (1) + selected *n*-alkane (2) binary systems at 323 K. Symbols: experimental data for (◆) *n*-butane,[2] (○) *n*-heptane,[5] (*) *n*-octane,[50] and (+) *n*-nonane.[8] Lines: GCA-EOS predictions.

carbon atom less than the transition that was observed with the R-23 and *n*-alkane homologues series. Since there are no experimental data available, it is difficult to confirm that this is the correct result. Nonetheless, given the good description of the phase transformation at constant temperature shown in Figures 7 and 8, one can expect fairly reliable model predictions for this series.

4. CONCLUSIONS

Light fluorinated refrigerants show interesting critical properties and have been investigated for novel supercritical fluid extraction technologies. A predictive thermodynamic model was proposed as a useful tool to be able to assess the applicability of these compounds. In this work, the GCA-EOS was applied in the modeling of phase equilibrium data for binary systems of R-23 or R-116 with alkanes and thus its ability to predict the phase behavior of these refrigerants has been extended to combinations with alkanes. The models were tested against experimentally measured phase equilibrium data for systems spanning the ranges of C_2 to C_{11} alkanes, and at temperature ranges between 193 and 343 K. Special attention was given to the representation of the transformation of the phase equilibria in the development of the multiphase predictive model. In the case of mixtures containing R-23, the model can predict the change in the van Konynenberg and Scott system type of phase behavior with an increase in the alkyl chain length to a fair degree of accuracy. The deviation between the predicted and experimental transition point was less than one carbon atom, with both the experimental and the predicted phase type transition occurring between *n*-hexane and *n*-heptane. As no data describing the critical end points of the R-116 + alkane systems are available, the phase type transition prediction by the GCA-EOS of between *n*-pentane and *n*-hexane was not verified experimentally. The parametrization obtained for R-23 and R-116 mixtures exhibited deviations in bubble pressure of approximately 2% and 4%, respectively. The GCA-EOS also correctly predicted the liquid−liquid immiscibility for the series. In all, the GCA-EOS gives a good description of the phase behavior of R-23 or R-116 with *n*-alkanes.

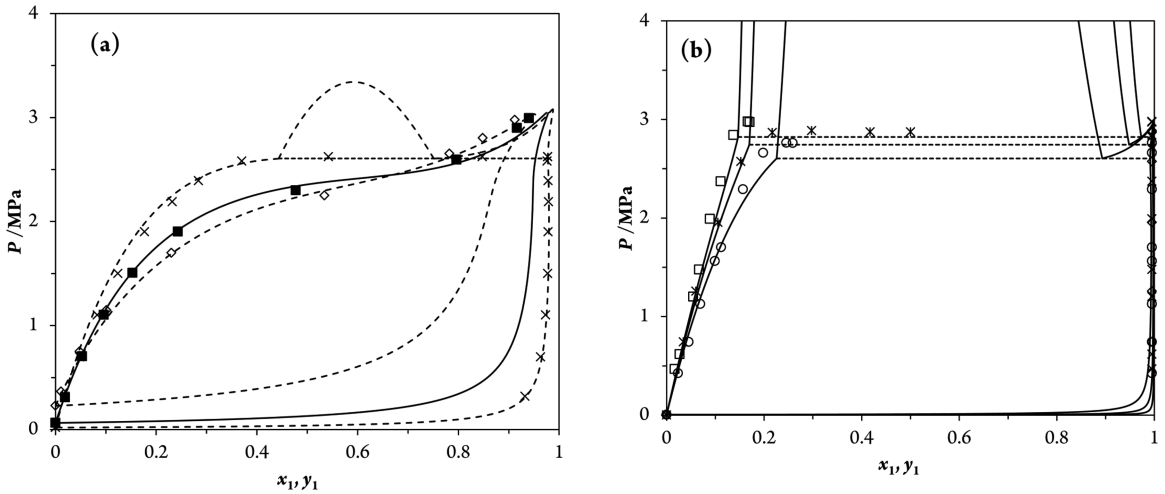

Figure 7. Phase behavior of R-116 (1) + alkane (2) binary systems at (a) T = 296 K and (b) T = 293 K. Symbols: experimental data for (◇) *n*-butane,[2] (■) *n*-pentane,[3] (×) *n*-hexane,[3] (○) *n*-heptane,[5] (*) *n*-octane,[50] and (□) *n*-decane.[8] Lines: solid and dashed, GCA-EOS correlation and prediction, respectively (this work); dotted, predicted VLLE (this work).

DOI: 10.1021/acs.iecr.8b01933
Ind. Eng. Chem. Res. XXXX, XXX, XXX−XXX

AUTHOR INFORMATION

Corresponding Author

*S. Pereda. E-mail: spereda@plapiqui.edu.ar.

ORCID

Mark D. Williams-Wynn: 0000-0002-9751-5419
Francisco Adrián Sánchez: 0000-0002-0666-4014
Selva Pereda: 0000-0002-2320-4298
Deresh Ramjugernath: 0000-0003-3447-7846

Notes

The authors declare no competing financial interest.

ACKNOWLEDGMENTS

The authors acknowledge the financial support of the MINCyT-DST Bilateral Cooperation Program SA/13/06, which made this collaboration possible. M. Williams-Wynn, P. Naidoo and D. Ramjugernath acknowledge the support of the National Research Foundation (NRF) of South Africa under the South African Research Chair Initiative (SARChI) of the Department of Science and Technology. The opinions expressed, and conclusions arrived at, are those of these authors, and are not necessarily to be attributed to the NRF. F. A. Sánchez and S. Pereda acknowledge the financial support granted by the Consejo Nacional de Investigaciones Cientificas y Técnicas (PIP 112 2015 010 856), the Ministerio de Ciencia, Tecnología e Innovación Productiva (MINCYT, PICT 2016 0907), and Universidad Nacional del Sur (PGI - 24/M133).

NOMENCLATURE

A	Helmholtz free energy
ARD(Z)	absolute relative deviation $\left\|1 - \frac{Z_{calc}}{Z_{exp}}\right\|$
AAD(Z)	average absolute deviation in variable Z: $\frac{1}{N}\sum_i^N \|Z_{exp,i} - Z_{calc,i}\|$
AARD(Z)%	average absolute relative deviation in variable Z: $\frac{100}{N}\sum_i^N \left\|1 - \frac{Z_{calc,i}}{Z_{exp,i}}\right\|$
a	van der Waals attractive parameter
d_{ci}	effective hard sphere diameter of component i evaluated at T_c
g_j	group energy per surface segment of group j
HC	hydrocarbon
HFC	hydrofluorocarbon
LLE	liquid−liquid equilibria
N	number of experimental points of each data set
NC	number of components in the mixture
NG	number of attractive groups in the mixture
NGA	number of associating groups in the mixture
n	total number of moles
n_i	number of moles of compound i
M_i	total number of associating sites in group i
P	pressure
q_j	number of surface segments of group j
R	universal gas constant
T	temperature
T_{ci}	critical temperature of component i
V	total volume of the mixture
VLE	vapor−liquid equilibria
VLLE	vapor−liquid−liquid equilibria
X_{ki}	fraction of nonbonded associating sites of type k in group i
x_i	molar composition in liquid phase of component i
y_i	molar composition in vapor phase of component i
Z	dummy variable

GreekSymbols

α_{ij}	nonrandomness parameter between groups i and j
$\Delta_{ki,lj}$	association strength between site k of group i and site l of group j
$\varepsilon_{ki,lj}$	energy of association between site k of group i and site l of group j
$\kappa_{ki,lj}$	volume of association between site k of group i and site l of group j
ν_{ij}	number of attractive groups j in compound i
ν_{ij}^*	number of associating groups j in compound i

REFERENCES

(1) Ramjugernath, D.; Valtz, A.; Coquelet, C.; Richon, D. Isothermal Vapor−Liquid Equilibrium Data for the Hexafluoroethane (R116) + Propane System at Temperatures from (263 to 323) K. *J. Chem. Eng. Data* **2009**, *54*, 1292−1296.

(2) Ramjugernath, D.; Valtz, A.; Richon, D.; Williams-Wynn, M. D.; Coquelet, C. Isothermal Vapor−Liquid Equilibrium Data for the Hexafluoroethane (R116) + n-Butane System at Temperatures from 273 to 323 K. *J. Chem. Eng. Data* **2017**, *62*, 3483−3487.

(3) Ramjugernath, D.; Valtz, A.; Richon, D.; Williams-Wynn, M. D.; Coquelet, C. Isothermal Vapour-Liquid Equilibrium Data for Binary Mixtures of Hexafluoroethane (R116) + n-Pentane or n-Hexane at Temperatures from (288 to 297) K. *J. Chem. Eng. Data* **2018**, *63*, 1228.

(4) Williams-Wynn, M. D.; Naidoo, P.; Ramjugernath, D. Isothermal (vapour + liquid) equilibrium data for binary systems of (n-hexane + CO2 or CHF3). *J. Chem. Thermodyn.* **2016**, *94*, 31−42.

(5) Williams-Wynn, M. D.; Naidoo, P.; Ramjugernath, D. Isothermal vapour-liquid equilibrium data for the binary systems of (CHF3 or C2F6) and n-heptane. *J. Chem. Thermodyn.* **2016**, *102*, 237−247.

(6) Williams-Wynn, M. D.; El Abbadi, J.; Valtz, A.; Kovacs, E.; Houriez, C.; Naidoo, P.; Coquelet, C.; Ramjugernath, D. Experimental determination of the critical loci for R-23 + (n-propane or n-hexane) and R-116 + n-propane binary mixtures. *J. Chem. Thermodyn.* **2017**, *108*, 84−96.

(7) Williams-Wynn, M. D.; Naidoo, P.; Ramjugernath, D. Isothermal vapour-liquid equilibrium data for binary systems of (CHF3 or C2F6) with (1-hexene or 3-methylpentane). *J. Chem. Thermodyn.* **2018**, *121*, 79−90.

(8) Williams-Wynn, M. D.; Naidoo, P.; Ramjugernath, D. Isothermal vapour-liquid equilibrium data for the binary systems of CHF3 with (n-nonane, n-decane, or n-undecane) and (C2F6 + n-decane). *Fluid Phase Equilib.* **2018**, *464*, 64−78.

(9) Dobbs, J. M.; Wong, J. M.; Johnston, K. P. Nonpolar co-solvents for solubility enhancement in supercritical fluid carbon dioxide. *J. Chem. Eng. Data* **1986**, *31*, 303−308.

(10) Kordikowski, A.; Schneider, G. M. Fluid phase equilibria of binary and ternary mixtures of supercritical carbon dioxide with low-volatility organic substances up to 100 MPa and 393 K. *Fluid Phase Equilib.* **1993**, *90*, 149−162.

(11) Guilbot, P.; Valtz, A.; Legendre, H.; Richon, D. Rapid On-line Sampler Injector: a Reliable Tool for HT-HP Sampling and On-Line GC Analysis. *Analusis* **2000**, *28*, 426−431.

(12) González Prieto, M.; Sánchez, F. A.; Pereda, S. Multiphase Equilibria Modeling with GCA-EoS. Part I: Carbon Dioxide with the Homologous Series of Alkanes up to 36 Carbons. *Ind. Eng. Chem. Res.* **2015**, *54*, 12415−12427.

(13) González Prieto, M.; Sánchez, F. A.; Pereda, S. Multiphase Equilibria Modeling with GCA-EoS. Part II: Carbon Dioxide with the Homologous Series of Alcohols. *J. Chem. Eng. Data* **2018**, *63*, 920.

(14) Polishuk, I.; Wisniak, J.; Segura, H. Simultaneous prediction of the critical and sub-critical phase behavior in mixtures using equation of state I. Carbon dioxide-alkanols. *Chem. Eng. Sci.* **2001**, *56*, 6485−6510.

DOI: 10.1021/acs.iecr.8b01933
Ind. Eng. Chem. Res. XXXX, XXX, XXX−XXX

(15) Polishuk, I.; Wisniak, J.; Segura, H. Estimation of Liquid−Liquid−Vapor Equilibria Using Predictive EOS Models. 1. Carbon Dioxide−n-Alkanes. *J. Phys. Chem. B* **2003**, *107*, 1864−1874.
(16) Polishuk, I.; Wisniak, J.; Segura, H. Simultaneous prediction of the critical and sub-critical phase behavior in mixtures using equations of state II. Carbon dioxide-heavy n-alkanes. *Chem. Eng. Sci.* **2003**, *58*, 2529−2550.
(17) Cismondi, M.; Rodríguez-Reartes, S. B.; Milanesio, J. M.; Zabaloy, M. S. Phase equilibria of CO 2 + n-alkane binary systems in wide ranges of conditions: Development of predictive correlations based on cubic mixing rules. *Ind. Eng. Chem. Res.* **2012**, *51*, 6232−6250.
(18) García, J.; Lugo, L.; Fernández, J. Phase Equilibria, PVT Behavior, and Critical Phenomena in Carbon Dioxide + n-Alkane Mixtures Using the Perturbed-Chain Statistical Associating Fluid Theory Approach. *Ind. Eng. Chem. Res.* **2004**, *43*, 8345−8353.
(19) Llovell, F.; Vega, L. F. Global Fluid Phase Equilibria and Critical Phenomena of Selected Mixtures Using the Crossover Soft-SAFT Equation. *J. Phys. Chem. B* **2006**, *110*, 1350−1362.
(20) Polishuk, I. Simultaneous Prediction of the Critical and Subcritical Phase Behavior in Mixtures of Perfluoromethane (1)−Alkanes (2). *Ind. Eng. Chem. Res.* **2006**, *45*, 6765−6769.
(21) Sánchez, F. A.; Pereda, S.; Brignole, E. A. GCA-EoS: A SAFT group contribution model—Extension to mixtures containing aromatic hydrocarbons and associating compounds. *Fluid Phase Equilib.* **2011**, *306*, 112−123.
(22) Espinosa, S.; Diaz, S.; Brignole, E. A. Thermodynamic Modeling and Process Optimization of Supercritical Fluid Fractionation of Fish Oil Fatty Acid Ethyl Esters. *Ind. Eng. Chem. Res.* **2002**, *41*, 1516−1527.
(23) Espinosa, S.; Diaz, M. S.; Brignole, E. A. Food additives obtained by supercritical extraction from natural sources. *J. Supercrit. Fluids* **2008**, *45*, 213−219.
(24) Gros, H. P.; Bottini, S.; Brignole, E. A. A group contribution equation of state for associating mixtures. *Fluid Phase Equilib.* **1996**, *116*, 537−544.
(25) Carnahan, N. F.; Starling, K. E. Equation of State for Nonattracting Rigid Spheres. *J. Chem. Phys.* **1969**, *51*, 635−636.
(26) Mansoori, G. A.; Leland, T. W. Statistical thermodynamics of mixtures. A new version for the theory of conformal solution. *J. Chem. Soc., Faraday Trans. 2* **1972**, *68*, 320−344.
(27) Renon, H.; Prausnitz, J. M. Local Compositions in Thermodynamic Excess Functions for Liquid Mixtures. *AIChE J.* **1968**, *14*, 135−144.
(28) Fredenslund, A.; Gmehling, J.; Rasmussen, P. Chapter 4-The UNIFAC group-contribution method. In *Vapor-liquid Equilibria Using UNIFAC*; Elsevier, 1977; pp 27−64.
(29) Abrams, D. S.; Prausnitz, J. M. Statistical thermodynamics of liquid mixtures: A new expression for the excess Gibbs energy of partly or completely miscible systems. *AIChE J.* **1975**, *21*, 116−128.
(30) Chapman, W. G.; Gubbins, K. E.; Jackson, G.; Radosz, M. New reference equation of state for associating liquids. *Ind. Eng. Chem. Res.* **1990**, *29*, 1709−1721.
(31) Skjold-Jørgensen, S. Gas solubility calculations. II. Application of a new group-contribution equation of state. *Fluid Phase Equilib.* **1984**, *16*, 317−351.
(32) Skjold-Joergensen, S. Group contribution equation of state (GC-EOS): a predictive method for phase equilibrium computations over wide ranges of temperature and pressures up to 30 MPa. *Ind. Eng. Chem. Res.* **1988**, *27*, 110−118.
(33) DIPPR801-Database. *Thermophysical Properties Database*, **1998**.
(34) Hou, Y. C.; Martin, J. J. Physical and thermodynamic properties of trifluoromethane. *AIChE J.* **1959**, *5*, 125−129.
(35) Rasskazov, D. S.; Petrov, E. K.; Spiridonov, G. A.; Ushmajkin, E. R. Investigation of P-V-T Data of Freon 31. *Teplofiz. Svoistva Veshchestv Mater.* **1975**, *8*, 4−16.
(36) Hori, K.; Okazaki, S.; Uematsu, M.; Watanabe, K. In *An Experimental Study of Thermodynamic Properties of Trifluoromethane, 8th Symp. Thermophys. Prop., Gaithersburg*; Sengers, J. V., Ed.; ASME: Gaithersburg, MD, 1982; pp 370−376.
(37) Timoshenko, N. I.; Kholodov, E. P.; Yamnov, A. L.; Tatarinova, T. A. Refractive Index, Polarization and Density of Freon 26. In *Teplofiz. Svoistva Veshchestv Mater.*; Rabinovich, V. A., Ed.; Standards Publ.: Moskow, 1975; Vol. *8*, pp 17−39.
(38) Ju, M.; Yun, Y.; Shin, M. S.; Kim, H. (Vapour & liquid) equilibria of the trifluoromethane (HFC-23) & propane, and trifluoromethane (HFC-23) & n-butane systems. *J. Chem. Thermodyn.* **2009**, *41*, 1339−1342.
(39) Kim, K. Y. Calorimetric studies on argon and hexafluoroethane and a generalized correlation of maxima in isobaric heat capacity. *Ph.D. Dissertation*; University of Michigan, Ann Arbor, MI, USA, 1974.
(40) Kijima, J.; Saikawa, K.; Watanabe, K.; Oguchi, K.; Tanishita, I. In *Experimental study of thermodynamic properties of hexafluoroethane (R116), Proc. Symp. Thermophys. Prop., 7th, New York*; Cezairliyan, A., Ed.; ASME: New York, 1977; p 480.
(41) Kleiber, M. Vapor-liquid equilibria of binary refrigerant mixtures containing propylene or R134a. *Fluid Phase Equilib.* **1994**, *92*, 149−194.
(42) Kao, C.-P. C.; Miller, R. N. Vapor Pressures of Hexafluoroethane and Octafluorocyclobutane. *J. Chem. Eng. Data* **2000**, *45*, 295−297.
(43) Valtz, A.; Coquelet, C.; Richon, D. Vapor-liquid equilibrium data for the hexafluoroethane + carbon dioxide system at temperatures from 253 to 297 K and pressures up to 6.5 MPa. *Fluid Phase Equilib.* **2007**, *258*, 179−185.
(44) Soria, T. M.; Andreatta, A. E.; Pereda, S.; Bottini, S. B. Thermodynamic modeling of phase equilibria in biorefineries. *Fluid Phase Equilib.* **2011**, *302*, 1−9.
(45) Zhang, Y.; Gong, M.; Zhu, H.; Wu, J. Vapor-liquid equilibrium data for the ethane + trifluoromethane system at temperatures from (188.31 to 243.76) K. *J. Chem. Eng. Data* **2006**, *51*, 1411−1414.
(46) Lim, J. S.; Park, J.-Y.; Lee, B. G.; Kim, J.-D. Phase Equilibria of Chlorofluorocarbon Alternative Refrigerant Mixtures. Binary Systems of Trifluoromethane + Isobutane at 283.15 and 293.15 K and 1,1,1-Trifluoroethane + Isobutane at 323.15 and 333.15 K. *J. Chem. Eng. Data* **2000**, *45*, 734−737.
(47) Zhang, Y.; Gong, M.-Q.; Zhu, H.-B.; Wu, J.-F. Vapor−liquid equilibrium measurements and correlations for an azeotropic system of ethane + hexafluoroethane. *Fluid Phase Equilib.* **2006**, *240*, 73−78.
(48) Dahmen, N.; Schneider, G. M. Phase separation in binary mixtures of trifluoromethane with propane, butane and xenon at low temperatures between 200 and 280 K, and at pressures up to 200 MPa. *Fluid Phase Equilib.* **1993**, *87*, 295−308.
(49) Sako, T.; Nakazawa, N.; Sugeta, T.; Sato, M.; Okubo, T.; Suzuki, M.; Hakuta, T.; Wakabayashi, K. High Pressure Vapor-Liquid Equilibria for Supercritical Trifluoromethane and C5-Hydrocarbons Systems. *Sekiyu Gakkaishi* **1989**, *32*, 75−81.
(50) Williams-Wynn, M. D.; Naidoo, P.; Ramjugernath, D. Isothermal vapour-liquid equilibrium data for the binary systems of (CHF3 + n-Octane) and (C2F6 + n-Octane). unpublished data
(51) van Konynenburg, P. H.; Scott, R. L. Critical Lines and Phase Equilibria in Binary Van Der Waals Mixtures. *Philos. Trans. R. Soc., A* **1980**, *298*, 495−540.
(52) Poot, W.; de Loos, W. Liquid-liquid-vapour equilibria in binary and quasi-binary systems of CHF3 with n-alkanes, phenylalkanes and alkanols. *Phys. Chem. Chem. Phys.* **1999**, *1*, 4293−4297.
(53) Peters, C. J.; Gauter, K. Occurrence of Holes in Ternary Fluid Multiphase Systems of Near-Critical Carbon Dioxide and Certain Solutes. *Chem. Rev.* **1999**, *99*, 419−432.
(54) Raeissi, S.; Gauter, K.; Peters, C. J. Fluid multiphase behavior in quasi-binary mixtures of carbon dioxide and certain 1-alkanols. *Fluid Phase Equilib.* **1998**, *147*, 239−249.
(55) Wirths, M.; Schneider, G. M. High-pressure phase studies on fluid binary mixtures of hydrocarbons with tetrafluoromethane and trifluoromethane between 273 and 630 K and up to 250 MPa. *Fluid Phase Equilib.* **1985**, *21*, 257−278.

DOI: 10.1021/acs.iecr.8b01933
Ind. Eng. Chem. Res. XXXX, XXX, XXX−XXX